Received: 13 February 2023 | Revised: 30 May 2023 | Accepted: 16 June 2023

DOI: 10.1111/gcb.16885

Global Change Biology WILEY

RESEARCH ARTICLE

Global distribution and climatic controls of natural mountain treelines

Xinyue He[1,2] | Xin Jiang[1] | Dominick V. Spracklen[2] | Joseph Holden[3] | Eryuan Liang[4,5] | Hongyan Liu[6] | Chongyang Xu[6] | Jianhui Du[7] | Kai Zhu[8,9] | Paul R. Elsen[10] | Zhenzhong Zeng[1]

[1]School of Environmental Science and Engineering, Southern University of Science and Technology, Shenzhen, China

[2]School of Earth and Environment, University of Leeds, Leeds, UK

[3]School of Geography, University of Leeds, Leeds, UK

[4]Key Laboratory of Alpine Ecology, Institute of Tibetan Plateau Research, Chinese Academy of Sciences, Beijing, China

[5]CAS Center for Excellence in Tibetan Plateau Earth Sciences, Beijing, China

[6]College of Urban and Environmental Science and MOE Laboratory for Earth Surface Processes, Peking University, Beijing, China

[7]School of Geography and Planning, Sun Yat-Sen University, Guangzhou, China

[8]Department of Environmental Studies, University of California, Santa Cruz, California, USA

[9]Institute for Global Change Biology and School for Environment and Sustainability, University of Michigan, Ann Arbor, Michigan, USA

[10]Wildlife Conservation Society, Global Conservation Program, Bronx, New York, USA

Correspondence
Zhenzhong Zeng, School of Environmental Science and Engineering, Southern University of Science and Technology, Shenzhen, China.
Email: zengzz@sustech.edu.cn

Funding information
National Natural Science Foundation of China, Grant/Award Number: 42071022; Southern University of Science and Technology, Grant/Award Number: 29/Y01296122, 29/Y01296222 and 29/Y01296602

Abstract

Mountain treelines are thought to be sensitive to climate change. However, how climate impacts mountain treelines is not yet fully understood as treelines may also be affected by other human activities. Here, we focus on "closed-loop" mountain treelines (CLMT) that completely encircle a mountain and are less likely to have been influenced by human land-use change. We detect a total length of ~916,425 km of CLMT across 243 mountain ranges globally and reveal a bimodal latitudinal distribution of treeline elevations with higher treeline elevations occurring at greater distances from the coast. Spatially, we find that temperature is the main climatic driver of treeline elevation in boreal and tropical regions, whereas precipitation drives CLMT position in temperate zones. Temporally, we show that 70% of CLMT have moved upward, with a mean shift rate of 1.2 m/year over the first decade of the 21st century. CLMT are shifting fastest in the tropics (mean of 3.1 m/year), but with greater variability. Our work provides a new mountain treeline database that isolates climate impacts from other anthropogenic pressures, and has important implications for biodiversity, natural resources, and ecosystem adaptation in a changing climate.

KEYWORDS
alpine area, climate, forest boundary, mountain ecosystems, tree cover, treeline

1 | INTRODUCTION

The mountain treeline is the upper altitudinal limit of tree growth toward the top of mountains, a transitional zone from forests to treeless alpine vegetation (Körner & Paulsen, 2004). Treeline ecotones play important environmental roles, including as habitats for endemic species and by contributing to water supply (Grace, 1989). Mountain treelines are important indicators of the impact of climate change on upland ecosystems (Lu et al., 2021; Verrall & Pickering, 2020) as they are strongly associated with growing season lengths and minimum daily temperatures (Paulsen & Körner, 2014). Consequently, as a response to global warming, mountain treelines are expected to shift upward as high elevations become more favorable for tree establishment under a changing climate (Du et al., 2018; Holtmeier & Broll, 2005). Furthermore, treeline shifts give rise to novel high-elevation vegetation patterns and could redefine habitable area for forest-dependent species in a warmer future world (Bolton et al., 2018; Mohapatra et al., 2019). However, the treelines in many mountain regions have been heavily altered by land-use change and land-use management (Ameztegui et al., 2016; Gehrig-Fasel et al., 2007). Such land-use-driven treelines are generally lower than the elevation of the local theoretical climatic treelines, making it difficult to isolate potential influences of climate on treeline position and obscuring the impact of climate change on treeline shifts. Therefore, accurate and reproducible detection of natural mountain treelines and their shifts are of great importance to understanding global climate change and the associated response of vegetation dynamics in alpine areas in natural systems.

Previous studies reporting local treeline sites have mainly relied on field investigation (Elliott & Cowell, 2015; Liang et al., 2014; Sigdel et al., 2018; Wardle & Coleman, 1992). While such studies have enhanced our understanding of treeline patterns, a key limitation of field-based studies is sparse geographic coverage. Remote sensing can overcome such a limitation by providing globally consistent coverage, but the determination of treeline positions only through visually interpreting satellite imagery (Irl et al., 2016; Karger et al., 2019; Paulsen & Körner, 2014) is time-consuming and labor-intensive at large spatial scales. Recently, regional attempts to combine remote sensing data with automated image processing techniques have emerged (Birre et al., 2023; Wang et al., 2022; Wei et al., 2020; Xu et al., 2020), but inconsistent analytical approaches and treeline definitions complicate regional comparisons and make it difficult to generalize global patterns. Early assessment at the global scale suggested that low temperatures limited tree growth at treelines (Körner & Paulsen, 2004), but there is also regional evidence that tree growth at the treeline does not increase under global warming due to moisture limitations (Camarero et al., 2021; Liang et al., 2014; Lyu et al., 2019). A generalizable pattern of the climatic limiting factors of global treelines is still lacking.

The aforementioned challenges and limitations associated with delineating treelines and determining climatic influences on treeline positions have hindered our understanding of the global impact of climate on treelines in natural systems. To address this issue, we focused on "closed-loop" mountain treelines (CLMT)—treelines with a continuous band of tree cover around a mountain. Such systems are less likely to have been influenced by land-use change. By focusing on this subset of treelines, we are better able to exclude treelines that may be impacted by topographic constraints or anthropogenic land use in order to isolate the effects of climate on mountain treelines in natural systems. An advance over previous studies that only provide a handful of data points for each treeline is a complete depiction of treeline at 30 m resolution. Our approach allows us to calculate the treeline elevation around the entire treeline, providing unprecedented detail on the variability of treeline elevation at the local scale. More importantly, using CLMT as a proxy for natural treelines with little influence from land-use change allows us to make a new and more robust assessment of how natural treelines are responding to changes in climate.

Here, we map closed-loop treelines in mountain regions globally in 2000 based on remote sensing, via integrating a high-resolution tree cover map (Hansen et al., 2013) with a digital elevation model at the same spatial resolution (Tachikawa et al., 2011). For this purpose, we develop a novel automatic detection algorithm that can produce consistent characterizations of CLMT across space. Our detection of mountain treeline is based on tree cover data that consider trees as any vegetation taller than 5 m (Hansen et al., 2013), using a 5% tree cover threshold to delineate forested and non-forested areas. The algorithm starts from the highest elevation point for each mountain range and generates a forest boundary map from which we extract the closed-loop treelines. To further ensure that our CLMT are natural treelines that are not impacted by anthropogenic disturbances, we conduct a manual inspection of high-resolution imagery to remove treelines with any indication of anthropogenic land use and restrict our analysis to regions where the human footprint is low (Mu et al., 2022). To understand which bioclimatic factors control the position of natural mountain treelines from global to local scales, we use the gradient boosting decision trees (GBDT) model (Friedman, 2001) to calculate the feature importance of each temperature or precipitation variable. Furthermore, we map the new natural treeline positions in 2010 using the same algorithm above and the amount of tree cover in 2010 (Hansen et al., 2013) to explore the shifting of mountain treelines in natural systems.

2 | METHODS

2.1 | Tree canopy cover data

We used a high-resolution remote sensing global map of tree canopy cover for the year 2000 (Hansen et al., 2013) to delineate forested and non-forested areas. The dataset was produced at a 30 m resolution based on multiple types of forest sample data and spectral curves of Landsat time series using a decision tree method (Hansen et al., 2013). To test which tree cover threshold is suitable for treeline mapping, we undertook a sensitivity analysis with different thresholds in mountains, finding there is little difference among different

thresholds from 0% to 10% (examples refer to Figures S1–S3). Thus, we took the mean value of 0%–10%, namely 5%, as the tree cover threshold, and define the treeline to be the transition zone above which tree cover is ≤5% and below which tree cover is >5%. We then binary-classified the tree canopy cover data using the threshold, assigning a value of 1 for the alpine land zone (the area above treeline) with tree cover ≤5% (non-forested area) and 0 for pixels with greater than 5% tree cover (forested area).

2.2 | Topography data

We combined global mountain polygons with a high-resolution digital elevation model to restrict the search area of mountain treelines. Mountain boundaries were collected from the Global Mountain Biodiversity Assessment (GMBA) inventory (version 1.2; Körner et al., 2017). The GMBA inventory delineated global mountains into discrete regions (polygons) based on topographic ruggedness metrics and expert delineation (Körner et al., 2017). The elevation information in mountains was provided by the Advanced Spaceborne Thermal Emission and Reflection Radiometer Global Digital Elevation Model (version 3; Tachikawa et al., 2011) at a spatial resolution of 30 m.

2.3 | Iterative mountain treeline extraction algorithm

We developed an algorithm to automatically detect CLMT (Figure S4). We first determined the coordinates of the highest peak within each mountain region. The algorithm starts at this peak point if it is within the alpine area that is non-forested, then expands outward (i.e., downslope), and determines all other pixels of the image that are connected to the point and equivalent (marked as "1"). The eight neighborhood region of the pixel $I(x, y)$ is expressed as:

$$R8 = \{(x + i, y + j); i, j \in (-1, 1)\}, \quad (1)$$

where I, j are integers. In the collection of the eight neighborhood pixels, if $I(x, y) = I(x + i, y + j)$, there are connected relationships. The connected domain generated by this method is the connected alpine area. Because the algorithm determines the starting search point, we marked only one connected domain (namely the treeline zone) after one iteration.

To accelerate the efficiency of the algorithm, we set search blocks to determine the full altitudinal range of treelines within mountain ranges (Figure S4). Specifically, the first round of the search takes the highest point of the mountain as the center and the buffer zone with a side length of R as the search area for the treeline. After testing, the square area with 8000 rows/ranks (side length R about 240 km) covered most alpine areas of mountains. For some of the mountaintops larger than this range, we expanded the side length to ~720 km to ensure that all close-loop mountain treelines of the world's mountaintops were covered.

There may be multiple treelines within a mountain range because a mountain may have multiple peaks. To account for this, we next searched for the second highest starting point (i.e., the highest point of the unsearched part) and repeated the process until the selected highest point was covered by forests (tree cover >5%).

After each iteration, the loops that were determined to be "open" were removed. Focusing only on closed treeline loops generated from the algorithm, we then visually inspected all loops using Google Earth (with spatial resolution ranging from 15 m to ~15 cm) to further exclude treelines with apparent signs of anthropogenic disturbances, such as roads, buildings, or croplands and removed the part of water bodies (i.e., pixels that were determined to be water). Last, we filled all the holes in the closed-loop polygons using the "imfill" function and extracted the edges of the binary images using the "bwperim" function in Matlab R2019a to obtain the CLMT positions.

To validate the robustness of the elevational distribution of CLMT derived from satellite images, at the pixel level, we used an independent validation dataset by manual interpretation using Google Earth's high-resolution images. We randomly produced 100 validation samples at a spatial resolution of 30 m. On a larger scale, we validated our CLMT database by comparison with in situ measures ($n = 62$; Table S1). For each treeline site, we corresponded it to the closest treeline loop detected in this study and compared its elevation with the range of the corresponding treeline loop.

2.4 | Climate data

Considering the effect of climatic lag effects on treelines (Harsch et al., 2009), we used the climate data from WorldClim (version 2.1; Fick & Hijmans, 2017), which provided the average for the years 1970–2000 at a resolution of 30 s (~1 km^2), to understand which climate variables are important in controlling treeline elevations. We used bioclimatic variables, which were derived from monthly temperature and precipitation. A total of eight temperature variables and eight precipitation variables were included, representing annual trends, seasonality, and extreme or limiting environmental factors. They are annual mean temperature (annual T), temperature seasonality (T seasonality; calculated as the standard deviation of the monthly mean temperatures, then multiply by 100), the maximum temperature of the warmest month (maximum T), the minimum temperature of the coldest month (minimum T), mean temperature of the wettest quarter (wet season T), mean temperature of the driest quarter (dry season T), mean temperature of the warmest quarter (warm season T), mean temperature of the coldest quarter (cold season T), annual precipitation (annual P), precipitation of the wettest month (maximum P), precipitation of the driest month (minimum P), precipitation seasonality (P seasonality; calculated as the coefficient of variation, which is the ratio of the standard deviation to the mean), precipitation of the wettest quarter (wet season P), precipitation of the driest quarter (dry season P), precipitation of the warmest quarter (warm season P), and precipitation of the coldest quarter (cold season P). A "quarter" here refers to any consecutive 3 months. For

example, the coldest quarter consists of the 3 months that are colder than any other set of three consecutive months. For each pixel determined to be on a CLMT, we extracted the values of all 16 climate variables.

2.5 | GBDT model

We applied a GBDT method to model the treeline elevation as a function of climate factors. The GBDT model is a type of tree model with good interpretability for feature values (Friedman, 2001), which assembles and iterates over multiple regression trees, with the values of the negative gradient of the loss function in the model as an approximation of the residuals of the lifting tree algorithm in the regression problem (Ke et al., 2017). It is flexible in handling large amounts of data and often performs well in dealing with complex relationships in data (Ke et al., 2017). The GBDT initializes a weak learner, estimating a constant value of the loss of function minimization, and then creates decision trees according to the datasets and performs iterative training on them. Next, it calculates the negative gradient for loss of function (residuals) corresponding to each tree, fits a regression tree to the residuals to obtain the leaf node region of the m-th tree, and minimizes loss of function by estimating the values of all leaf node regions using a linear search. Last, GBDT repeats the above steps until the target evaluation indicator is optimal. Using this model, we calculated the feature importance of each variable and determined the dependent correlations for each factor after the model was built. The GBDT analysis was undertaken in Python 3.7 with the "sklearn.ensemble" module.

We carried out the GBDT analyses at global and local scales, as well as separately for different climatic belts (i.e., boreal, temperate, and tropical regions). At the global and regional scales, we considered each treeline loop as a sample, namely, using the mean of treeline elevation in each loop for the analysis. A total of 1690 samples (treeline loops) were used for the global model. At the local scale, we regarded one treeline pixel as a sample. Hence, in each treeline loop, the repeated GBDT model represents the local effect of climate factors on treeline positions.

2.6 | Mountain treeline shift rate

We mapped the new treeline positions in 2010 based on the global 2010 tree cover data (Hansen et al., 2013; Potapov et al., 2015), which is an update of the 2000 tree cover product. Using this dataset, we reran the algorithm around treelines to detect the new closed-loop treelines in 2010. Starting from the highest elevation point we detected before, we expanded the rectangular area of the original treeline around by 10 km as the search area. Then, we manually checked the results from the 1690 treeline loops to (i) exclude treelines without closed loops; (ii) isolate examples of "broken treeline loops" and restrict them to corresponding areas in 2000 and 2010 (Figure S5); and (iii) remove outliers (>95th percentile of both increasing and decreasing rates) to avoid the inclusion of any special cases with extremely steep changes. This filtering resulted in 1110 treeline loops in 2010 (65.7% of all treelines initially assessed) being available for analysis of the treeline change. The main reason for the reduction in number of treeline loops between 2000 and 2010 is that some of the closed-loop treelines detected in 2000 did not form closed loops in 2010. We then calculated the mean elevation of closed-loop treelines in 2010 and the corresponding treelines in 2000 and used the difference to represent the treeline change over the 10-year period. The treeline shift rate (m/year) at each treeline loop was calculated as follows:

$$\text{shift rate} = \frac{\text{mean elevation 2010} - \text{mean elevation 2000}}{\text{10 years}}. \quad (2)$$

3 | RESULTS

3.1 | A map of global CLMT

We detected 27,468,662 CLMT positions (pixels at 30 m resolution) across 243 mountain ranges globally. The total length of CLMT we detected is ~916,425 km. Those treeline pixels form 1690 treeline loops covering all continents except Antarctica, ranging from 64°N (Khrebet Polyarnyy) to 46°S (Princess Mountains), with mean elevations spanning from 489 ± 283 m on Khrebet Chayatyn to 4528 ± 104 m on Ruwenzori. The average length of these treeline loops is 542 km, and the average alpine land area above them is 142 km^2. To visualize global patterns of the elevation of CLMT, we calculated the mean elevation for each treeline loop and plotted their locations using the mean latitude and longitude of treeline pixels at 30 m resolution in each loop (Figure 1a). The CLMT derived from satellite tree cover data are consistent with fine resolution remote sensing images available on Google Earth (Figure 1b–g). At the pixel level, the CLMT showed good agreement with manually interpreted data at 30 m resolution ($R^2 = .96$; Figure S6). On a larger scale, the validity of our CLMT database was further supported by corroboration against in situ measures from previous studies ($n = 62$ measurements; Table S1), which fall within the elevation range of treeline loops ($R^2 = .98$; Figure S7).

We found a bimodal pattern for the CLMT elevation along latitude, with peaks at the equator and ~25°N (Figure 2a). Between 0° and 10°N/S, the elevation of CLMT is symmetrical in the northern and southern hemispheres, but beyond this range, treeline elevations in the northern hemisphere are higher than those in the southern hemisphere at equivalent latitudes (Figure 2a), which is attributed to the oceanic influence on a smaller southern landmass (Cieraad et al., 2014). Our global CLMT distribution is consistent with previous global assessments (Körner, 1998; Irl et al., 2016; Testolin et al., 2020), though there are some differences. In the tropics, the elevation of CLMT reaches up to 3500 m (Figure 2), a lower elevation than in a recent global assessment by Testolin et al. (2020) that reported tropical treelines higher than 4000 m. This discrepancy may be due to our strict definition of trees, >5 m height, as well as the exclusion of some unilateral and non-closed

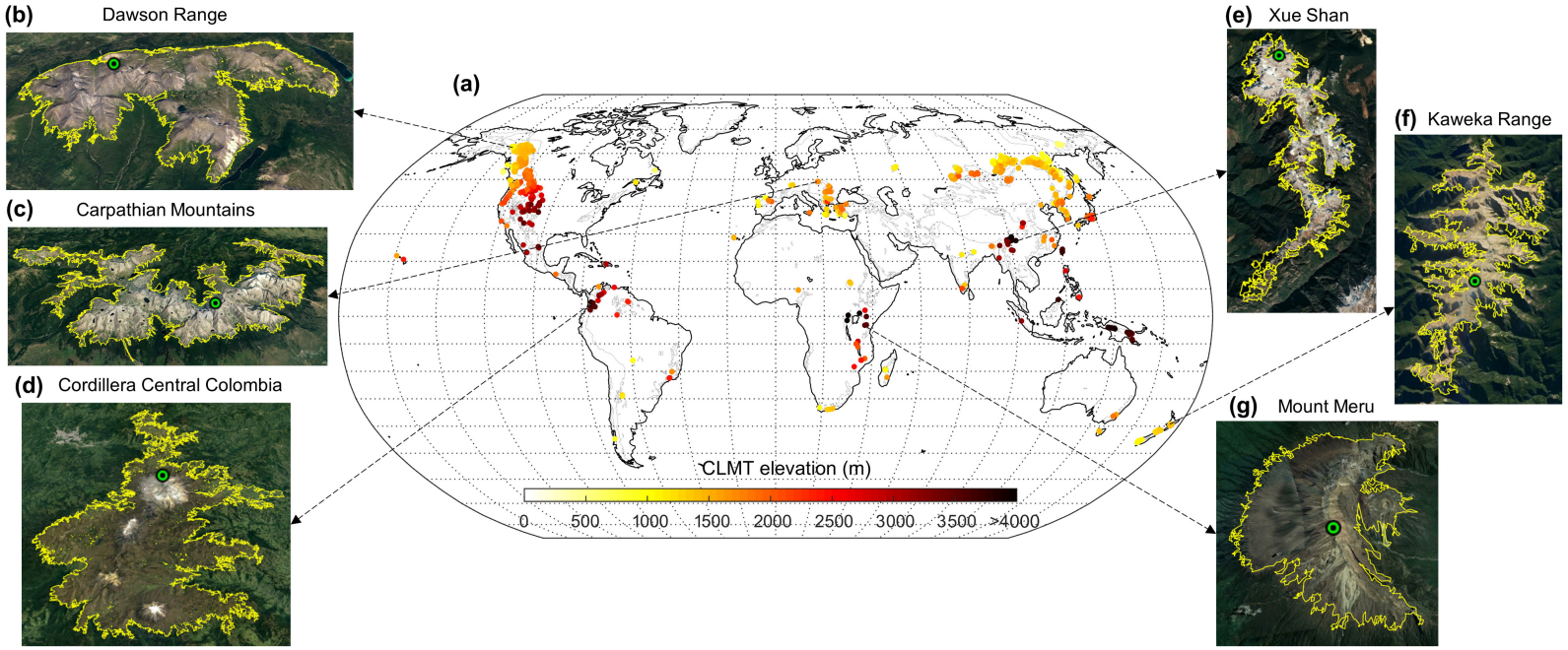

FIGURE 1 Global distribution of closed-loop mountain treeline (CLMT) elevation. To improve readability, plot (a) is based on the mean value of each treeline loop (at each 30-m pixel). Gray boundaries indicate mountain regions defined by GMBA inventory data. (b–g) Examples of CLMT extraction results superimposed with Google Earth images. The yellow line represents the position of the treeline, and the green circle shows the highest elevation point that formed the starting point of each search by the treeline algorithm.

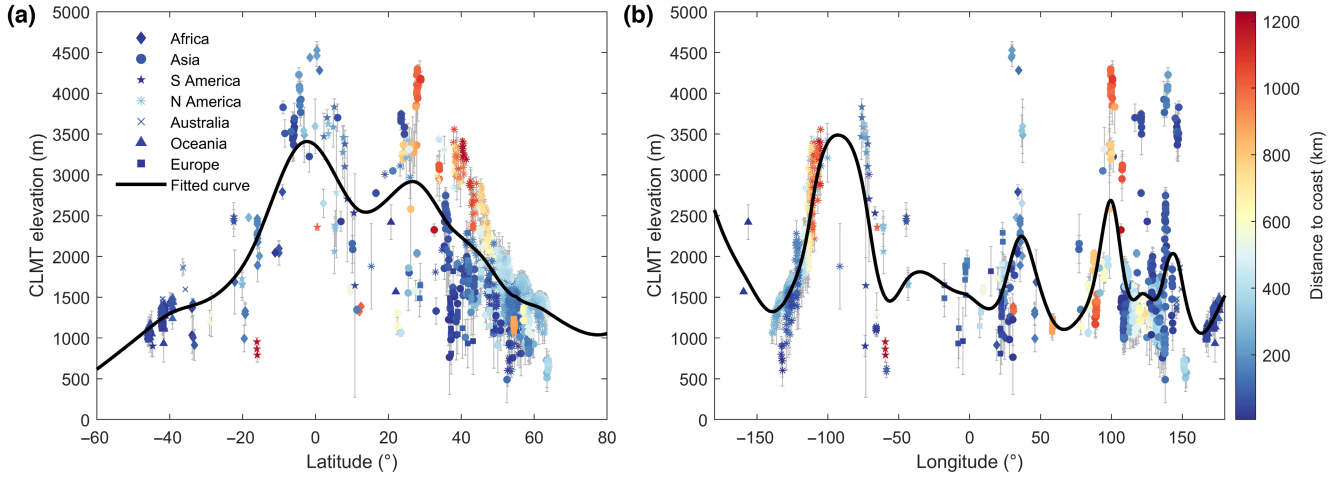

FIGURE 2 Global latitudinal (a) and longitudinal (b) variation of closed-loop mountain treeline (CLMT) elevation. Different symbols represent different regions and colors represent the distance to the coast. The data points show the mean elevation of all of the pixels in the CLMT. The error bar is the elevation range of the corresponding treeline loop.

treelines in high mountains. At low latitude (especially at 0–20° N), there is large variation in the range of CLMT elevation (Figure 2a). Among different continents, South America has a large CLMT elevation range variation. At 50–60° N and 20–30° N, many mountains in Asia and North America have similar treeline elevations, whereas there is a rather different behavior at 30–50° N where treelines in North America are higher than those in Europe and Asia (Figure 2a). To help understand what causes this behavior, we calculated the distance to the coast for each treeline. We found lower treelines in coastal mountains at the same latitude (Figure 2a) as has been suggested in the literature (Irl et al., 2016), which can be largely attributed to the thermodynamic effect of large high-elevation landmasses (Karger et al., 2019). At 30–60° N, mountains close to the coast have lower treelines than their latitude might suggest (i.e., fall below the fitted curve; Figure 2a). Similarly, along with longitude decreasing from 150 to 100° W, treeline elevations in North America increase due to an increase in the distance to the coast (Figure 2b).

3.2 | Climatic determinants of CLMT

We found that *T* seasonality, cold season *P*, and warm season *T* predict nearly 60% of the spatial distribution of CLMT globally (Figure 3a). We then assessed how the three leading factors modulated the elevation of CLMT spatially. The results showed the abrupt transition of CLMT elevation occurring at the *T* seasonality threshold of ~9°C, but attenuated transitions in areas where *T* seasonality exceeded 10°C (Figure S8a). Similarly, there is a CLMT elevation gradient that is spatially driven by cold season *P*, with abrupt transitions occurring at the thresholds of 320 mm and 450 mm along the gradient of cold season *P* (Figure S8b). By contrast, we did not find such a dramatic transition of CLMT elevation along the warm season *T* gradient (Figure S8c).

Collectively, temperature-related factors (64%) are more important than precipitation-related factors for limiting CLMT elevations on a global scale (Figure 3a). In different latitudinal belts, temperature-related factors are most important in boreal and tropical regions, especially the temperature of the warmest and the wettest quarters, respectively, while precipitation dominates the CLMT elevation in temperate regions (Figure 3b–d). We found that *T* seasonality is the most important individual factor (30%) at global scale, whereas its importance is lower than 10% for boreal and tropical regions (Figure 3). These patterns may be because thermal limitation to growth at treelines during the summer is most critical in the cold boreal regions, while in the tropics where temperature is high throughout the year, temperature of the wettest season plays a key role in limiting tree growth at treelines. Our results confirm the importance of temperature during the warm part of the year in the boreal zone (Jobbágy & Jackson, 2000), but suggest that precipitation is more important than temperature in temperate regions. It agrees with climatic sensitivity of tree growth in the Norther Hemisphere (Gao et al., 2022). Especially under dry environmental conditions, moisture availability is crucial to limiting tree growth in the treeline ecotone (Liang et al., 2014; Ren et al., 2018).

Our study provides vastly more data points for each treeline compared to previous global assessments (Jobbágy & Jackson, 2000; Körner & Paulsen, 2004), allowing us to explore for the first time what controls treeline position at a local scale. We found that temperature remains the dominant explanation for the altitudinal variation of 76% of the treeline within a single treeline loop with similar climatic conditions (Figure S9).

3.3 | Shifts in CLMT

Between 2000 and 2010, mountain treelines shifted upward at 777 of the 1110 treeline loops (70%) and downward at 333 treeline

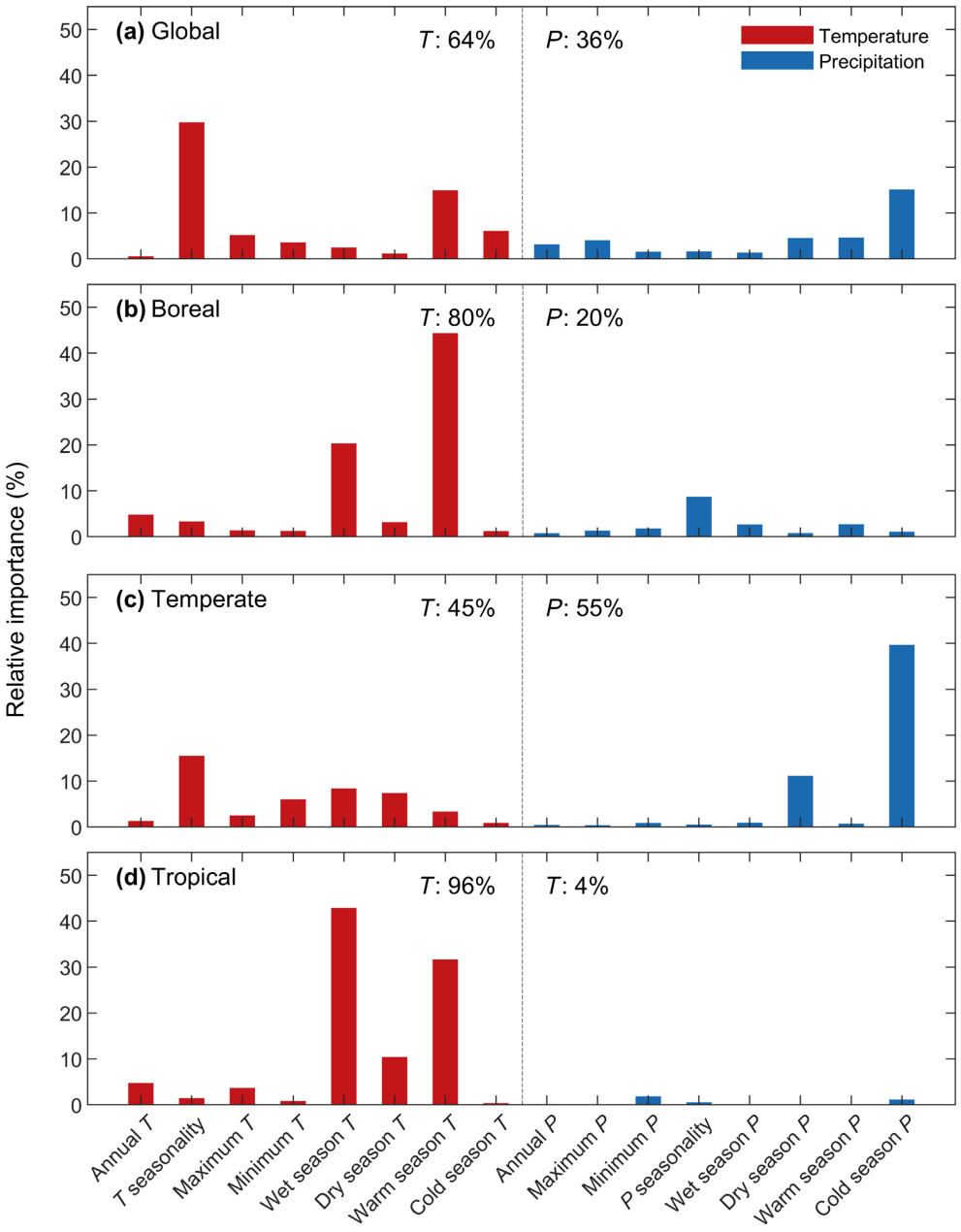

FIGURE 3 Climate drivers controlling the variability in treeline elevation for the globe (a), boreal (≥50° N, b), temperate (23.5°–50° N/S, c) and tropical (23.5° N–23.5° S, d) regions.

loops (Figure 4a). The mean global treeline shift rate was an upward shift of 1.2 m/year, which is consistent with case studies of treeline change, with rates >1 m/year reported in the literature (Table S2). A synthesis of treeline shift rates reported in the literature suggests the rate was 0.67 m/year before 1970 compared to 4.36 m/year after 1970 and 6.16 m/year after 2000 (Figure S10; Table S2). This provides evidence that the rate of change in treeline elevation is accelerating, possibly due to recent rapid climate change (Bolton et al., 2018). Treeline shift rates in the tropics (mean of 3.1 m/year) were higher than those in boreal and temperate regions (Figure 4b). The faster changes in the topics could be related to hydrothermal conditions: in the tropics, higher temperature and more abundant precipitation bring a longer growing season, which naturally favors the growth of seedlings and young trees. By contrast, there is a slight downward shift in temperate regions (an average of −0.5 m/year), where the position of the treeline is dominated by precipitation (Figure 3c). This could be due to decreasing precipitation in some mountain areas of the temperate zone, for example, in northern China (Piao et al., 2010).

Although the tropical CLMT have the fastest shift rates, their variability is the largest, ranging from −10.2 to 16.9 m/year (Figure 4b). In the tropics, treeline shift rates greater than 10 m/year in the mountains of Malawi, Papua New Guinea, and Indonesia may reflect a more extreme trend in these tropical systems. In other regions, there are also some treelines that have shifted much more than expected (>10 m/year; Figure 4b): In boreal

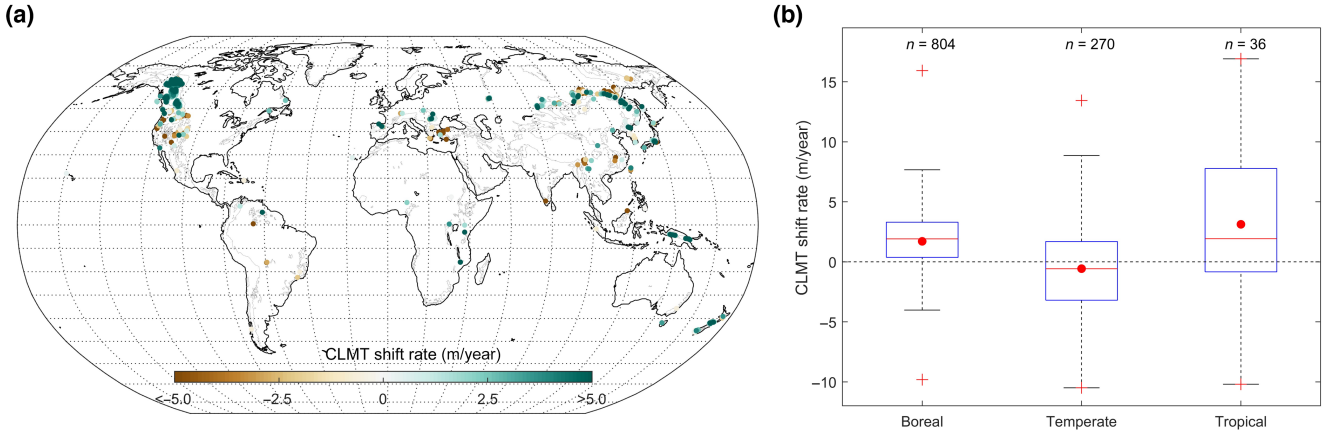

FIGURE 4 Closed-loop mountain treeline (CLMT) shift rate during 2000–2010. (a) Spatial pattern of CLMT shift rate. (b) Box-plot showing CLMT shift rate in boreal (≥50° N), temperate (23.5°–50° N/S), and tropical (23.5° N–23.5° S) regions (central line: median; red dot: mean; box: 25th and 75th percentiles, respectively; error bar: maximum and minimum whisker values; +: maximum and minimum values). The black dashed line is the zero line. Numbers of the studied CLMT are shown above the boxes.

regions, these expectations are mainly in Russia and Canada; in temperate regions, they are geographically concentrated in East Asia (North Korea, Japan, and China). On the contrary, there are also cases of treelines receding at a high rate, possibly driven by fire in some areas, either through the physical destruction of trees that acts to lower the existing treelines, or through the destruction of seedlings established upslope that acts to prevent treeline advances (Kim & Lee, 2015). For example, treelines have significantly receded in the western United States where climate and vegetation are favorable for fire (Seven Devils Mountains, Swan Range, etc.; Figure 4a).

In addition, independent analysis for the changes in annual maximum Normalized Difference Vegetation Index (NDVI) at CLMT that we identified for the year 2000 shows the NDVI has significantly increased by 3.3% by 2020, at a rate of 0.0012 per year ($p < .01$; Figure S11a). There are significant positive trends in NDVI at treeline zones in boreal, temperate, and tropical regions during 2000–2020 ($p < .01$), and tropical areas have the highest rate, approaching 0.0016 per year (Figure S11b). The increase in NDVI occurred at most treeline zones (~90%; Figure S11c). This greening at the treeline may also be conducive to upward movement of the treeline in the future.

4 | DISCUSSION

4.1 | Comparison of treeline datasets before and after considering human footprint

Although we have examined CLMT by manual interpretation to remove anthropogenic treelines, we further conduct a stricter assessment of human pressures to check whether our results would still be impacted by human activity. We used a global Human Footprint dataset (Mu et al., 2022) and found 83% of our CLMT in wilderness (Human Footprint <1) or in highly intact areas (Human Footprint <4). We then removed those treelines with human footprint values ≥4, reran the analysis with the higher human footprint values excluded, and updated all the results above (Figures S12–S14). By comparing these new results with those using the whole dataset, we found a similar pattern along latitude and longitude gradients (Figure 2; Figure S12). The results regarding climate dominants (Figure 3; Figure S13) and treeline shift rates (Figure 4b; Figure S14) were also consistent using either approach. Thus, the additional criterion to further focus our analysis on treelines with no human disturbance does not alter our overall results or conclusions, and further confirms that our CLMT product can well represent the change and pattern of climatic treelines.

4.2 | Implications of treeline shifts for carbon, biodiversity, and hydrology

Changing treeline position can affect the carbon cycle, biodiversity, and hydrological processes in mountain environments. Mountain treelines moving upward to higher elevations increase woody biomass at and above the treeline, accumulating carbon and increasing their ability to act as carbon sinks (Lopatin et al., 2006; Tarnocai et al., 2009). However, such increases may be offset by increases in soil respiration, leading to a net loss of ecosystem carbon (Hartley et al., 2012; Wilmking et al., 2006). The ascent of mountain treelines also substantially influences biodiversity patterns at high elevations, with enhanced habitat loss of endemic alpine species within a narrow range of mountains (Wang et al., 2022) and potential expansion of habitat for forest-dependent species whose upper range limits coincide with the treeline ecotones (Elsen et al., 2017). For alpine species isolated at the top of mountains, upward treeline shifts could increase the risk of extinction, where there is not enough room for the alpine zone to move upward under future climate change (Dirnböck et al., 2011). In Siberia, for example, we show many treelines have shifted upward (Figure 4b), inevitably reducing the area of the tundra, which is rich in floristic and

species diversity and supports indigenous land use types. The expansion of Siberian forests has been predicted to continue, thus causing huge losses of tundra in the future (Kruse & Herzschuh, 2022). While we focused here on treeline shifts in areas with minimal human impacts, treeline ascent in areas with pronounced human disturbance will further hinder species' ability to track vegetation changes and likely lead to more pronounced population declines (Elsen et al., 2020; Feeley & Silman, 2010). There are many instances with high pressure in high-elevation areas, especially from burning, grazing, and wood harvesting (Bader et al., 2008; Jiménez-García et al., 2021). The combined impact of shifting treelines and human disturbances may also affect local livelihoods and act as a double-blow for sensitive alpine species. In addition, tree expansions into the formerly treeless area may alter downstream water supply. Recent advances of the treeline have decreased the area of alpine tundra, thereby affecting its critical role as a reservoir of freshwater resources and in water release (Barredo et al., 2020).

4.3 | Uncertainties and caveats

To isolate the impacts of climate on treelines, our analysis identifies CLMT that completely encircle a mountain. However, focusing on this kind of treelines could omit some climate-related treelines as climatic treelines may not be in a closed-loop shape in some cases. We acknowledge that our CLMT database does not include all climatic treelines, but is a subset of climatic treelines that specifically form a closed loop, because these enable us to analyze climatic determinants with greater confidence. We also note that tree cover can increase in various ways, either through new or existing trees growing above the 5 m height threshold, or existing trees having increased canopy cover. However, our analysis is based on the definition of treeline according to remotely sensed tree cover, and we used this definition to assess treeline position at two time periods and assess change. While our analysis period is short and errors will exist at a pixel scale, our global detection of a shifting treeline provides an early indication of climate-induced changes that need to be carefully monitored in the future. To reduce uncertainties and further advance our understanding of treeline dynamics, future studies require more high-resolution remote sensing products for a longer period and more field data in alpine treeline zones for cross-validation.

5 | CONCLUSION

Our study develops a novel remote sensing-based algorithm to map closed-loop treelines across global mountain regions, isolating the effects of climate on treeline position. Our approach provides a globally consistent way of detecting and monitoring closed-loop treelines around mountains, which are more likely to reflect natural systems with minimal impact of land-use change. Focusing on these closed-loop treelines as a proxy for natural treelines allows us to isolate the impacts of climate and climate change on the elevation distribution and change of treelines. We found temperature was the dominant control on natural treelines both at a global and local scale. Our results indicated an upward migration of treelines over the period 2000–2010 in boreal and tropical regions but a slight downward shift in temperate zones. Our new findings and the global closed-loop mountain treeline database produced in this study also provide a useful tool for biodiversity and carbon assessments, ecological modeling, and analyses of adaptation of species to future climate change.

AUTHOR CONTRIBUTIONS

Xinyue He, Zhenzhong Zeng, Dominick V. Spracklen, and Joseph Holden designed the research; Xinyue He performed the analysis and wrote the draft; and all the authors contributed to the interpretation of the results and the writing of the paper.

ACKNOWLEDGMENTS

X.H. was funded by a PhD scholarship from Southern University of Science and Technology hosted jointly with the University of Leeds. Z.Z. was supported by the National Natural Science Foundation of China (no. 42071022) and the start-up fund provided by Southern University of Science and Technology (no. 29/Y01296122; 29/Y01296222; 29/Y01296602). We thank Hansen/UMD/Google/USGS/NASA for providing the high-resolution tree cover data; NASA and Japan's Ministry of Economy, Trade and Industry for providing the elevation data; Körner for providing the GMBA inventory; Fick and Hijmans for providing WorldClim data; and Google Earth for providing very high-resolution satellite imagery.

CONFLICT OF INTEREST STATEMENT

The authors declare no competing interests.

DATA AVAILABILITY STATEMENT

The global tree cover data in 2000 are available at https://earthenginepartners.appspot.com/science-2013-global-forest/download_v1.7.html and the tree cover data in 2010 are available at https://glad.umd.edu/Potapov/TCC_2010/. The ASTER elevation data are available at https://earthdata.nasa.gov/. The GMBA inventory is available at https://ilias.unibe.ch/goto_ilias3_unibe_cat_1000515.html. The WorldClim climate data are available at https://www.worldclim.org/data/worldclim21.html. The MODIS combined 16-day NDVI is available at https://developers.google.com/earth-engine/datasets/catalog/MODIS_MCD43A4_006_NDVI. The scripts used to generate the figures are available in GitHub at https://github.com/hexinyue33/treeline. The global closed-loop mountain treeline (CLMT) database developed in this study can be accessed through https://hexinyue33.users.earthengine.app/view/clmt.

ORCID

Xinyue He https://orcid.org/0000-0002-2214-9338
Xin Jiang https://orcid.org/0000-0003-4141-1538
Dominick V. Spracklen https://orcid.org/0000-0002-7551-4597
Joseph Holden https://orcid.org/0000-0002-1108-4831
Eryuan Liang https://orcid.org/0000-0002-8003-4264

Hongyan Liu https://orcid.org/0000-0002-6721-4439
Jianhui Du https://orcid.org/0000-0003-2905-9797
Kai Zhu https://orcid.org/0000-0003-1587-3317
Paul R. Elsen https://orcid.org/0000-0002-9953-7961
Zhenzhong Zeng https://orcid.org/0000-0001-6851-2756

REFERENCES

Ameztegui, A., Coll, L., Brotons, L., & Ninot, J. M. (2016). Land-use legacies rather than climate change are driving the recent upward shift of the mountain tree line in the P yrenees. *Global Ecology and Biogeography*, *25*(3), 263–273. https://doi.org/10.1111/geb.12407

Bader, M. Y., Rietkerk, M., & Bregt, A. K. (2008). A simple spatial model exploring positive feedbacks at tropical alpine treelines. *Arctic, Antarctic, and Alpine Research*, *40*(2), 269–278. https://doi.org/10.1657/1523-0430(07-024)[BADER]2.0.CO;2

Barredo, J. I., Mauri, A., & Caudullo, G. (2020). Alpine tundra contraction under future warming scenarios in Europe. *Atmosphere*, *11*(7), 698. https://doi.org/10.3390/atmos11070698

Birre, D., Feuillet, T., Lagalis, R., Milian, J., Alexandre, F., Sheeren, D., Serrano-Notivoli, R., Vignal, M., & Bader, M. Y. (2023). A new method for quantifying treeline-ecotone change based on multiple spatial pattern dimensions. *Landscape Ecology*, *38*, 779–796. https://doi.org/10.1007/s10980-022-01589-4

Bolton, D. K., Coops, N. C., Hermosilla, T., Wulder, M. A., & White, J. C. (2018). Evidence of vegetation greening at alpine treeline ecotones: Three decades of Landsat spectral trends informed by lidar-derived vertical structure. *Environmental Research Letters*, *13*(8), 084022. https://doi.org/10.1088/1748-9326/aad5d2

Camarero, J. J., Gazol, A., Sánchez-Salguero, R., Fajardo, A., McIntire, E. J. B., Gutiérrez, E., Batllori, E., Boudreau, S., Carrer, M., Diez, J., Dufour-Tremblay, G., Gaire, N. P., Hofgaard, A., Jomelli, V., Kirdyanov, A. V., Lévesque, E., Liang, E., Linares, J. C., Mathisen, I. E., … Wilmking, M. (2021). Global fading of the temperature-growth coupling at alpine and polar treelines. *Global Change Biology*, *27*(9), 1879–1889. https://doi.org/10.1111/gcb.15530

Cieraad, E., McGlone, M. S., & Huntley, B. (2014). Southern hemisphere temperate tree lines are not climatically depressed. *Journal of Biogeography*, *41*(8), 1456–1466. https://doi.org/10.1111/jbi.12308

Dirnböck, T., Essl, F., & Rabitsch, W. (2011). Disproportional risk for habitat loss of high-altitude endemic species under climate change. *Global Change Biology*, *17*(2), 990–996. https://doi.org/10.1111/j.1365-2486.2010.02266.x

Du, H., Liu, J., Li, M.-H., Büntgen, U., Yang, Y., Wang, L., Wu, Z., & He, H. S. (2018). Warming-induced upward migration of the alpine treeline in the Changbai Mountains, northeast China. *Global Change Biology*, *24*(3), 1256–1266. https://doi.org/10.1111/gcb.13963

Elliott, G. P., & Cowell, C. M. (2015). Slope aspect mediates fine-scale tree establishment patterns at upper treeline during wet and dry periods of the 20th century. *Arctic, Antarctic, and Alpine Research*, *47*(4), 681–692. https://doi.org/10.1657/AAAR0014-025

Elsen, P. R., Monahan, W. B., & Merenlender, A. M. (2020). Topography and human pressure in mountain ranges alter expected species responses to climate change. *Nature Communications*, *11*(1), 1–10. https://doi.org/10.1038/s41467-020-15881-x

Elsen, P. R., Tingley, M. W., Kalyanaraman, R., Ramesh, K., & Wilcove, D. S. (2017). The role of competition, ecotones, and temperature in the elevational distribution of Himalayan birds. *Ecology*, *98*(2), 337–348. https://doi.org/10.1002/ecy.1669

Feeley, K. J., & Silman, M. R. (2010). Land-use and climate change effects on population size and extinction risk of Andean plants. *Global Change Biology*, *16*(12), 3215–3222. https://doi.org/10.1111/j.1365-2486.2010.02197.x

Fick, S. E., & Hijmans, R. J. (2017). WorldClim 2: New 1-km spatial resolution climate surfaces for global land areas. *International Journal of Climatology*, *37*(12), 4302–4315. https://doi.org/10.1002/joc.5086

Friedman, J. H. (2001). Greedy function approximation: A gradient boosting machine. *Annals of Statistics*, *29*, 1189–1232.

Gao, S., Liang, E., Liu, R., Babst, F., Camarero, J. J., Fu, Y. H., Piao, S., Rossi, S., Shen, M., Wang, T., & Peñuelas, J. (2022). An earlier start of the thermal growing season enhances tree growth in cold humid areas but not in dry areas. *Nature Ecology & Evolution*, *6*(4), 397–404. https://doi.org/10.1038/s41559-022-01668-4

Gehrig-Fasel, J., Guisan, A., & Zimmermann, N. E. (2007). Tree line shifts in the Swiss Alps: Climate change or land abandonment? *Journal of Vegetation Science*, *18*, 571–582. https://doi.org/10.1111/j.1654-1103.2007.tb02571.x

Grace, J. (1989). Tree lines. *Philosophical Transactions of the Royal Society of London. B, Biological Sciences*, *324*(1223), 233–245.

Hansen, M. C., Potapov, P. V., Moore, R., Hancher, M., Turubanova, S. A., Tyukavina, A., Thau, D., Stehman, S. V., Goetz, S. J., & Loveland, T. R. (2013). High-resolution global maps of 21st-century forest cover change. *Science*, *342*(6160), 850–853. https://doi.org/10.1126/science.1244693

Harsch, M. A., Hulme, P. E., McGlone, M. S., & Duncan, R. P. (2009). Are treelines advancing? A global meta-analysis of treeline response to climate warming. *Ecology Letters*, *12*(10), 1040–1049. https://doi.org/10.1111/j.1461-0248.2009.01355.x

Hartley, I. P., Garnett, M. H., Sommerkorn, M., Hopkins, D. W., Fletcher, B. J., Sloan, V. L., Phoenix, G. K., & Wookey, P. A. (2012). A potential loss of carbon associated with greater plant growth in the European Arctic. *Nature Climate Change*, *2*(12), 875–879. https://doi.org/10.1038/nclimate1575

Holtmeier, F., & Broll, G. (2005). Sensitivity and response of northern hemisphere altitudinal and polar treelines to environmental change at landscape and local scales. *Global Ecology Biogeography*, *14*(5), 395–410. https://doi.org/10.1111/j.1466-822X.2005.00168.x

Irl, S. D., Anthelme, F., Harter, D. E., Jentsch, A., Lotter, E., Steinbauer, M. J., & Beierkuhnlein, C. (2016). Patterns of Island treeline elevation—A global perspective. *Ecography*, *39*(5), 427–436. https://doi.org/10.1111/ecog.01266

Jiménez-García, D., Li, X., Lira-Noriega, A., & Peterson, A. T. (2021). Upward shifts in elevational limits of forest and grassland for Mexican volcanoes over three decades. *Biotropica*, *53*, 798–807. https://doi.org/10.1111/btp.12942

Jobbágy, E. G., & Jackson, R. B. (2000). Global controls of forest line elevation in the northern and southern hemispheres. *Global Ecology Biogeography*, *9*(3), 253–268. https://doi.org/10.1046/j.1365-2699.2000.00162.x

Karger, D. N., Kessler, M., Conrad, O., Weigelt, P., Kreft, H., König, C., & Zimmermann, N. E. (2019). Why tree lines are lower on islands—Climatic and biogeographic effects hold the answer. *Global Ecology Biogeography*, *28*(6), 839–850. https://doi.org/10.1111/geb.12897

Ke, G., Meng, Q., Finley, T., Wang, T., Chen, W., Ma, W., Ye, Q., & Liu, T.-Y. (2017). Lightgbm: A highly efficient gradient boosting decision tree. *Advances in Neural Information Processing Systems*, *30*, 3146–3154.

Kim, J. W., & Lee, J. S. (2015). Dynamics of alpine treelines: Positive feedbacks and global, regional and local controls. *Journal of Ecology and Environment*, *38*(1), 1–14. https://doi.org/10.5141/ecoenv.2015.001

Körner, C. (1998). A re-assessment of high elevation treeline positions and their explanation. *Oecologia*, *115*, 445–459.

Körner, C., Jetz, W., Paulsen, J., Payne, D., Rudmann-Maurer, K., & Spehn, M. E. (2017). A global inventory of mountains for bio-geographical applications. *Alpine Botany*, *127*(1), 1–15. https://doi.org/10.1007/s00035-016-0182-6

Körner, C., & Paulsen, J. (2004). A world-wide study of high altitude treeline temperatures. *Journal of Biogeography*, *31*(5), 713–732. https://doi.org/10.1111/j.1365-2699.2003.01043.x

Kruse, S., & Herzschuh, U. (2022). Regional opportunities for tundra conservation in the next 1000 years. *eLife*, *11*, e75163. https://doi.org/10.7554/eLife.75163

Liang, E., Dawadi, B., Pederson, N., & Eckstein, D. (2014). Is the growth of birch at the upper timberline in the Himalayas limited by moisture or by temperature? *Ecology*, *95*(9), 2453–2465. https://doi.org/10.1890/13-1904.1

Lopatin, E., Kolström, T., & Spiecker, H. (2006). Determination of forest growth trends in Komi Republic (northwestern Russia): Combination of tree-ring analysis and remote sensing data. *Boreal Environment Research*, *11*, 341–353.

Lu, X., Liang, E., Wang, Y., Babst, F., & Camarero, J. J. (2021). Mountain treelines climb slowly despite rapid climate warming. *Global Ecology and Biogeography*, *30*(1), 305–315. https://doi.org/10.1111/geb.13214

Lyu, L., Zhang, Q. B., Pellatt, M. G., Büntgen, U., Li, M. H., & Cherubini, P. (2019). Drought limitation on tree growth at the Northern Hemisphere's highest tree line. *Dendrochronologia*, *53*, 40–47. https://doi.org/10.1016/j.dendro.2018.11.006

Mohapatra, J., Singh, C. P., Tripathi, O. P., & Pandya, H. A. (2019). Remote sensing of alpine treeline ecotone dynamics and phenology in Arunachal Pradesh Himalaya. *International Journal of Remote Sensing*, *40*(20), 7986–8009. https://doi.org/10.1080/01431161.2019.1608383

Mu, H., Li, X., Wen, Y., Huang, J., Du, P., Su, W., Miao, S., & Geng, M. (2022). A global record of annual terrestrial Human Footprint dataset from 2000 to 2018. *Scientific Data*, *9*(1), 176. https://doi.org/10.1038/s41597-022-01284-8

Paulsen, J., & Körner, C. (2014). A climate-based model to predict potential treeline position around the globe. *Alpine Botany*, *124*(1), 1–12. https://doi.org/10.1007/s00035-014-0124-0

Piao, S., Ciais, P., Huang, Y., Shen, Z., Peng, S., Li, J., Zhou, L., Liu, H., Ma, Y., Ding, Y., & Friedlingstein, P. (2010). The impacts of climate change on water resources and agriculture in China. *Nature*, *467*(7311), 43–51. https://doi.org/10.1038/nature09364

Potapov, P., Turubanova, S., Tyukavina, A., Krylov, A., McCarty, J., Radeloff, V., & Hansen, M. (2015). Eastern Europe's forest cover dynamics from 1985 to 2012 quantified from the full Landsat archive. *Remote Sensing of Environment*, *159*, 28–43. https://doi.org/10.1016/j.rse.2014.11.027

Ren, P., Rossi, S., Camarero, J. J., Ellison, A. M., Liang, E., & Peñuelas, J. (2018). Critical temperature and precipitation thresholds for the onset of xylogenesis of Juniperus przewalskii in a semi-arid area of the north-eastern Tibetan Plateau. *Annals of Botany*, *121*(4), 617–624. https://doi.org/10.1093/aob/mcx188

Sigdel, S. R., Wang, Y., Camarero, J. J., Zhu, H., Liang, E., & Peñuelas, J. (2018). Moisture-mediated responsiveness of treeline shifts to global warming in the Himalayas. *Global Change Biology*, *24*(11), 5549–5559. https://doi.org/10.1111/gcb.14428

Tachikawa, T., Hato, M., Kaku, M., & Iwasaki, A. (2011). Characteristics of ASTER GDEM version 2. In *2011 IEEE international geoscience and remote sensing symposium* (pp. 3657–3660). IEEE. https://doi.org/10.1109/IGARSS.2011.6050017

Tarnocai, C., Canadell, J. G., Schuur, E. A. G., Kuhry, P., Mazhitova, G., & Zimov, S. (2009). Soil organic carbon pools in the northern circumpolar permafrost region. *Global Biogeochemical Cycles*, *23*, GB2023. https://doi.org/10.1029/2008GB003327

Testolin, R., Attorre, F., & Jiménez-Alfaro, B. (2020). Global distribution and bioclimatic characterization of alpine biomes. *Ecography*, *43*(6), 779–788. https://doi.org/10.1111/ecog.05012

Verrall, B., & Pickering, C. M. (2020). Alpine vegetation in the context of climate change: A global review of past research and future directions. *Science of the Total Environment*, *748*, 141344. https://doi.org/10.1016/j.scitotenv.2020.141344

Wang, X., Wang, T., Xu, J., Shen, Z., Yang, Y., Chen, A., Wang, S., Liang, E., & Piao, S. (2022). Enhanced habitat loss of the Himalayan endemic flora driven by warming-forced upslope tree expansion. *Nature Ecology & Evolution*, *6*(7), 890–899. https://doi.org/10.1038/s41559-022-01774-3

Wardle, P., & Coleman, M. (1992). Evidence for rising upper limits of four native New Zealand forest trees. *New Zealand Journal of Botany*, *30*(3), 303–314. https://doi.org/10.1080/0028825X.1992.10412909

Wei, C., Karger, D. N., & Wilson, A. M. (2020). Spatial detection of alpine treeline ecotones in the Western United States. *Remote Sensing of Environment*, *240*, 111672. https://doi.org/10.1016/j.rse.2020.111672

Wilmking, M., Harden, J., & Tape, K. (2006). Effect of tree line advance on carbon storage in NW Alaska. *Journal of Geophysical Research*, *111*, 1–10. https://doi.org/10.1029/2005JG000074

Xu, D., Geng, Q., Jin, C., Xu, Z., & Xu, X. (2020). Tree line identification and dynamics under climate change in Wuyishan National Park based on Landsat images. *Remote Sensing*, *12*(18), 2890. https://doi.org/10.3390/rs12182890

SUPPORTING INFORMATION

Additional supporting information can be found online in the Supporting Information section at the end of this article.

How to cite this article: He, X., Jiang, X., Spracklen, D. V., Holden, J., Liang, E., Liu, H., Xu, C., Du, J., Zhu, K., Elsen, P. R., & Zeng, Z. (2023). Global distribution and climatic controls of natural mountain treelines. *Global Change Biology*, *00*, 1–11. https://doi.org/10.1111/gcb.16885